

# This is a self-archived version of an original article. This version may differ from the original in pagination and typographic details.

**Author(s):** Vandesande, Helena; Laajala, Mira; Kantoluoto, Tino; Ruokolainen, Visa; Lindberg, A. Michael; Marjomäki, Varpu

Title: Early entry events in Echovirus 30 infection

**Year:** 2020

**Version:** Accepted version (Final draft)

**Copyright:** © 2020 American Society for Microbiology.

Rights: In Copyright

**Rights url:** http://rightsstatements.org/page/InC/1.0/?language=en

# Please cite the original version:

Vandesande, H., Laajala, M., Kantoluoto, T., Ruokolainen, V., Lindberg, A. M., & Marjomäki, V. (2020). Early entry events in Echovirus 30 infection. Journal of Virology, 94(13), Article e00592-20. https://doi.org/10.1128/JVI.00592-20

Word count text:

# Downloaded from http://jvi.asm.org/ on April 15, 2020 at KIRJASTO KAUSIJULKAISUT

5355 words

# Early entry events in Echovirus 30 infection

JVI Accepted Manuscript Posted Online 15 April 2020

Copyright © 2020 American Society for Microbiology. All Rights Reserved.

J. Virol. doi:10.1128/JVI.00592-20

2		
3	Early e	entry events in Echovirus 30 infection
4		
5	Helena V	andesande <sup>1</sup> , Mira Laajala <sup>2</sup> , Tino Kantoluoto <sup>2</sup> , Visa Ruokolainen <sup>2</sup> , A. Michael Lindberg <sup>1</sup> ,
6	Varpu Ma	rjomäki <sup>2</sup>
7		
8	1 Li	nnaeus University, Department of Chemistry and Biomedical Sciences, Linnaeus University,
9	Ka	almar, Sweden
10	<sup>2</sup> Jy	väskylä University, Department of Biological and Environmental Science / Nanoscience
11	CE	enter, University of Jyväskylä, Jyväskylä, Finland
12		
13	Correspor	ndence: Varpu Marjomäki
14		Faculty of Mathematics and Science
15		Department of Biological and Environmental Science
16		Jyväskylä University
17		FI – 400 14 Jyväskylä
18		Tel.: +358 (0) 40 563 44 22
19		E – mail: <u>varpu.s.marjomaki@jyu.fi</u>
20		
21		
22		
23		
24		
25		
26		
27		
28		
29		
30		
31		
32		
33		
34		
35		
36	Word cour	nt abstract: 209 words

### **ABSTRACT**

38 39 40

41

42

43

44

45

46

47

48

49 50

51

52

53 54 Echovirus 30 (E30), a member of the enterovirus B species, is a major cause of viral meningitis, targeting children and adults alike. While it is a frequently isolated enterovirus and the cause of several outbreaks all over the world, suprisingly little is known regarding its entry and replication strategy within cells. In this study, we used E30 Bastianni (E30B) generated from an infectious cDNA clone in order to study early entry events during infection in human RD cells. E30B required the newly discovered Fc echovirus receptor (FcRn) for succesful infection, but not the Coxsackievirus and Adenovirus Receptor (CAR) or Decay-Accelerating Factor (DAF), although an interaction with DAF was observed. Double-stranded RNA replication intermediate was generated between 2 and 3 h postinfection (p.i.). and viral capsid production was initiated between 4 and 5 h p.i. The drugs affecting Rac1 (NSC 23766) and cholesterol (Filipin III) compromised infection, whereas bafilomycin A1, dyngo, U-73122, wortmannin and nocodazole did not, suggesting the virus follows an enterovirus-triggered macropinocytic pathway rather than the clathrin pathway. Colocalization with early endosomes and increased infection due to constitutively active Rab5 expression suggests some overlap and entry to classical early endosomes. Taken together, these results suggest that E30B induces an enterovirus entry pathway, leading to uncoating in early endosomes.

## **IMPORTANCE**

56 57

55

58

59

60

61

62

63

64

Echovirus 30 (E30) is a prevalent enterovirus causing regular outbreaks in both children and adults in different parts of the world. It is therefore surprising that relatively little is known of its infectious entry pathway. We set out to generate a cDNA clone and gradient-purified the virus in order to study the early entry events in human cells. We have recently studied other enterovirus B group viruses, like echovirus 1 (EV1) and coxsackievirus A9 (CVA9), and found many similarities between those viruses, allowing us to define a so-called "enterovirus entry pathway". Here, E30 is reminiscent of these viruses, e.g. by not relying on acidification for infectious entry. However, despite not using the clathrin entry pathway, E30 accumulates in classical early endosomes.

Downloaded from http://jvi.asm.org/ on April 15, 2020 at KIRJASTO KAUSIJULKAISUT

65 66	KEYWORDS
67	Enterovirus
68	Echovirus 30
69	Aseptic meningitis
70	Early entry

Downloaded from http://jvi.asm.org/ on April 15, 2020 at KIRJASTO KAUSIJULKAISUT

### INTRODUCTION

72 73

71

74

75

76

77

78

79

80

81 82

83

84

85

86

87

88

89

90

91

92

93

94

95

96

97

98

99

100

101

Meningeal inflammation lacking an identifiable bacterial origin is a common neurological syndrome known as aseptic meningitis. Its clinical course, however similar, is generally milder than that of its bacterial counterpart; nonetheless, viral meningitis occurs more frequently and leads to the hospitalisation of 26,000 to 42,000 people every year in the US alone, thus representing a significant economical and societal burden (1-3). Many different viruses can trigger the development of viral meningitis, such as herpesviruses, influenzaviruses, and arboviruses (4, 5). Since the introduction of the mumps, measles, and rubella (MMR) combination vaccine in 1988, however, non-polio enteroviruses have taken over as the leading cause of the disease, accounting for over 90 % of all cases in which the etiological agent has been identified (1, 4, 6-8). Among these, group B coxsackieviruses and echoviruses are the most commonly isolated types, in particular echovirus 30 (E30) (8).

E30, a picornavirus belonging to the Enterovirus B genus, is a frequently isolated, positive-sense RNA virus of approximately 7,500 nucleotides enclosed by a non-enveloped protein capsid. Outbreaks of E30-related aseptic meningitis have been recorded every 3 - 5 years in many regions of the world, including Europe, Asia, and the United States (9-15). E30 is the enterovirus type that, over time, has been most frequently reported in humans with aseptic meningitis, and has been demonstrated to form a phylogenetic cluster with other notable echoviruses such as echovirus 21 (E21), echovirus 25 (E25), and echovirus 29 (E29) (2, 16). Moreover, the 5' noncoding region of E30 shows between 68 % (coxsackievirus A24, CVA24) and 93 % (coxsackievirus B3, CVB3) homology with other human enteroviruses, and appears to contain some coxsackie B-like genomic features (17). Despite often being the subject of medical and epidemiological reports, E30 has been grievously overlooked with regards to its life cycle and infection mechanisms. Using an infectious E30 Bastianni (E30B) cDNA clone, this project aimed to study early events in the echovirus life cycle, as well as to pinpoint key cellular components necessary for viral entry into the host cell. We show that E30B represents a typical enterovirus B group virus using an enterovirus-triggered macropinocytic entry pathway leading to rapid replication which does not require endosomal acidification to facilitate infection. However, it sets itself apart from its closest enterovirus relatives by showing accumulation in classical early endosomes. Being the first report detailing the mechanism of early entry and infection by E30B, this study may open the door to a deeper understanding of the life cycle and infection mechanisms of this pathogen.

102 103

## **RESULTS**

104 105 106

107

108

109

110

E30B displays efficient replication and infection kinetics in human RD cells. E30B virus stocks were produced from a newly constructed cDNA clone, as described in the Materials and Methods. TEM visualisation of the negatively stained, gradient purified E30B revealed typical enteroviral particles, as E30B preparations consisted mainly of intact icosahedral viral particles with a low quantity of empty capsids (Fig. 1A,B). In order to visualise the entry and life cycle of E30B, we performed

112

113

114 115

116

117

118

119

120 121

122

123

124

125

126

127

128

129

130

131 132

133

134

135

136

137

138

139

140

141

142 143

144

145

146 147

148

149

immunolabeling of E30B infected RD and A549 cells during various time points post-infection (p.i.). Labeling of the replication intermediate using J2, an antibody specifically geared towards dsRNA, showed that the earliest signs of viral replication appeared between 2 and 3 h p.i. in both RD cells (Fig. 1C) and A549 cells (data not shown). Subsequent quantification of the dsRNA signal using a larger amount of cells from confocal images showed that dsRNA was already detectable at 2.5 h p.i., and the intensity of the signal increased exponentially as the infection progressed (Fig. 1D). Growth curve analysis through quantitative RT-PCR monitoring the E30B infection progression in RD

cells also showed a low viral load before 3 h p.i., as evidenced by the high qRT-PCR cycle threshold (C<sub>1</sub>) value, followed by an increase in intracellular E30B RNA starting from 4 h p.i., confirming the dsRNA IF labeling (Fig. 1E). These results indicated that E30B adapted extremely well to RD cell culture and reached a high viral titre.

E30B infection was also followed using confocal microscopy by labeling the capsid with antibodies against VP1. E30B capsid protein could be visualised using the monoclonal rhesus monkey antiserum from ATCC originally prepared against human E30 virus (Fig. 2). The vesicular label was scattered and mostly peripheral for the first 4 h p.i., after which the cytoplasmic, more widespread signal increased. The labeling was also performed with the monoclonal mouse antiserum (Clone 5-D8/1, DAKO) reactive against several members of the enterovirus B group virus VP1 capsid proteins, which showed a similar distribution in infected cells (data not shown). Together, these data support the notion that E30B appears to exhibit similar efficient replication and infection kinetics as other members of the enterovirus B genus (18, 19).

E30B uses DAF as its attachment receptor. Members of the CVB cluster within the enterovirus B genus utilise the Coxsackievirus and Adenovirus receptor (CAR) to attach to and enter their respective host cells (20-22). While some enteroviruses also interact with the Decay-Accelerating Factor (DAF) receptor, this interaction in itself is often insufficient for virus entry into the cell (23-25). We performed a radioactive E30B receptor binding assay to assess the propensity for attachment of E30B to CAR and DAF. Based on this experiment, the virus does not bind to CAR but preferentially attaches to the DAF - receptor, a feature that is in line with previous findings (Fig. 3) (23, 26, 27). CHO-cells stably transfected with CAR (CHO-CAR) or DAF (CHO-DAF) were confirmed for strong DAF or CAR expression, respectively, using immunofluorescence and FACS (data not shown).

It has recently been shown that CD64, the Fc receptor (FcRn), acts as a pan-receptor for all echoviruses, including E30 (28, 29). We therefore performed a double labeling using antibodies against FcRn and capsid antibodies during E30B infection. Despite the presence of FcRn in A549 cells, we found no difference in the distribution of the receptor in infected cells compared to noninfected cells. The receptor showed a small vesicular appearance in all studied timepoints. In addition, we found no apparent colocalization of E30B with FcRn at any infected timepoint (Fig. 4). This was confirmed by careful quantification of the colocalization using automatic thresholding for colocalization. The Manders' coefficient was kept at a maximum of 10 % in all studied timepoints, including in the non-infected control cells, suggesting that the colocalization was caused by the background noise.

As this was quite unexpected due to recent results on the importance of FcRn as an echoviral receptor also for E30B, we decided to perform siRNA knock-down of the receptors studied here: FcRn, DAF and CAR. Despite having no effect on the cellular distribution of FcRn during E30B infection, the siRNA treatment of FcRn completely abolished E30B infection in A549 cells (Fig. 5). In addition, siRNA knock-down of CAR or DAF, respectively, did not affect the infection of E30B. Furthermore, we used another enterovirus, namely CVB5, as a control, as it has been shown to use the CAR and DAF receptors, but not FcRn, during infection (21, 24, 29). Indeed, our results showed that, in contrast to E30B, CVB5 infection was not affected by FcRn knock-down, but instead, the infection was clearly decreased by CAR or DAF siRNA treatment (Fig. 5). Taken together, these results show that E30B requires FcRn for successful infection, although DAF, unlike CAR, may function as a co-receptor for attachment.

160 161 162

163

164 165

166

167

168

169

170

171

172

173

174

175

176

177

178

179

180

181 182

183

184

185

186

187

150

151

152

153 154

155

156

157

158 159

> Effects of pharmacological inhibitors on early E30B entry. Other members of the enterovirus B subgroup have been previously shown to prefer the non-clathrin pathway to enter their respective host cells (22, 30-32). Through the use of chemical inhibitors known to affect the action of several key elements of cell entry, we attempted to assess which cellular components or pathways are indispensable for virus infection and replication to occur. Subconfluent monolayers of RD cells were treated with the different compounds for 30 min prior to virus addition, after which the infection was allowed to proceed for 6 h at 37 °C. After incubation, the cells were fixed and labeled with a panenteroviral VP1 capsid protein antibody. Immunofluorescent labeling of the viral capsid allowed visual distinction between infected and uninfected cells using confocal microscopy. The entry inhibitor drug NSC 23766 (inhibiting Rac1) drastically reduced the pathogen's capacity for infection, suggesting that this cellular components is essential for virus entry. In contrast, phosphoinositide 3-kinases (PI3K), endosomal acidification, phospholipase C activation, dynamin, and microtubule (de) polymerisation appeared not to influence E30B infection, as evidenced by the use of wortmannin, bafilomycin A1, U-73122, Dyngo 4a, and nocodazole, respectively (Fig. 6).

Downloaded from http://jvi.asm.org/ on April 15, 2020 at KIRJASTO KAUSIJULKAISUT

None of the compounds significantly affected cell survival in the used concentration compared to a control group, as evidenced by the evaluation of the cell toxicity assay (Fig. 7). This indicated the observed cell deaths were natural rather than a toxic chemical effect.

To confirm the confocal microscopy data, the capacity of these drugs to interfere with viral replication was further evaluated by quantification of the amount of intracellular viral RNA using qPCR (Fig. 8). As previously shown, NSC 23766 affected RNA replication, confirming our previous microscopy results. The treatment with NSC 23766 prevented RNA replication, resulting in an amount of viral RNA that was below the detectable level.

In addition, the effect of the cholesterol modifying drug Filipin III on E30B infection was studied using quantitative RT-PCR (Fig. 9A). The results showed that filipin treatment decreased replication, as the C<sub>t</sub> value increased from 20 for the control infection to 25 for the filipin treatment, corresponding to a 30-fold decrease in viral RNA amount. The results also showed that the lowest effective concentration of filipin was not cytotoxic to RD cells (Fig. 9B).

188 189

191

192

193

194

195

196

197 198

199

200

201

202

203

204

205

206

207

208

209

210

211

212

213

214

215

216

217

218

219

220

221

222

223

224

225

226 227 228

229

E30B colocalizes with early endosomes during early entry. The early endosomes are a preferred sorting station for several incoming vesicles, regardless of the origin of the plasma membrane-derived vesicle. In our earlier studies with echovirus 1 (EV1) and coxsackievirus A9 (CVA9) we found negligible colocalization of the viruses with early endosomes (18, 33). Our results here with bafilomycin A1 and nocodazole showed that acidification of the endosomal structures and microtubule-dependent targeting of E30B to the perinuclear region was not necessary for infection. However, we were curious to find out if E30B would still enter the early sorting or early recycling endosomes; therefore, we infected RD cells with E30B and used confocal immunofluorescence microscopy to visualize possible colocalization of the virus with EEA1 for early sorting endosomes and the transferrin receptor for recycling early endosomes (Fig. 10). After an incubation period of 5 min colocalization of E30B with the endosomal markers was rather low; however, this colocalization increased dramatically after 30 min, suggesting that E30B does indeed invade the early endosomal compartments, but with delayed kinetics in comparison to cargo relying on clathrin-dependent entry. After 5 min, E30B colocalized to some extent both with internalized transferrin as well as with EEA1. Also, transferrin and EEA1 showed good colocalization of their signals, which is expected given that transferrin passes the sorting early endosomes on its way to recycling early endosomes. In contrast, as previously described, CVA9 did not colocalize with either of the endosomal markers, indicating that CVA9, unlike E30B, does not enter the early endosomal compartments at any time (18). Interestingly, after 30 min of E30B entry, there was much higher colocalization between transferrin and EEA1 and the volume of the colocalized structures had increased due to virus infection. This suggests that transferrin recycling and the overall dynamics of early endosomes were affected by the E30B infection. Due to the involvement of early endosomes in E30B infection, we investigated the role of Rab5 in E30B infection by transfecting RD cells with different Rab5 constructs (Fig. 11). This small GTPase is important for the dynamics of early endosomes, particularly for their homotypic fusion (34). In addition, Rab5 and some of its effectors have been shown to regulate macropinosome dynamics (35, 36). Our

Downloaded from http://jvi.asm.org/ on April 15, 2020 at KIRJASTO KAUSIJULKAISUT

experiment showed that E30B infection was approximately 40 % lower (p < 0.01) in cells transfected with a dominant-negative Rab5 construct (pEGFP-Rab5-S34N) compared to the wild type Rab5 control. In addition, overexpression of the constitutively active Rab5 gene markedly improved E30B infection as transfection with the constitutively active Rab5 (pEYFP-Rab5-Q79L) resulted in a circa 70 % increase of infection compared to the wild type Rab5 (p < 0.05). In contrast, the infection of CVA9 was less affected by the dominant-negative Rab5 (p < 0.05) and in comparison to E30B, constitutively active Rab5 decreased the infection of CVA9 which has also been previously shown (18). Altogether, these results further suggest that, in contrast to CVA9, E30B uses early endosomes as a route of entry.

### **DISCUSSION**

Despite its role as a principal cause of viral meningitis, and the consequent extensive epidemiological and diagnostic attention it has received, the life cycle and replication mechanics of E30 have long

231

232

233 234

235

236

237

238

239

240

241

242

243

244

245

246

247

248

249

250

251

252

253

254

255

256

257

258

259

260

261

262

263

264

265

266

267

268

been overlooked. Here, we report the development of a novel infectious cDNA clone - the first of its kind, to the best of our knowledge - which actively replicates and infects in cell culture, allowing us to study and investigate early entry events in E30 infection using immunofluorescence and confocal

Time-resolved analysis of the early infection progression suggested that E30B shows very similar infection and replication kinetics to other enterovirus B members, a notion that is supported by our findings regarding dsRNA production and initiation of viral replication (Fig. 1) (18, 19).

Members of the CVB cluster within the enterovirus B genus tend to favor the CAR - receptor to facilitate attachment and entry into their respective host cells (20-22). In some cases, the DAF receptor may function as a coreceptor for attachment, but this interaction in itself is often insufficient to establish infection (23-25). We found that E30B does not bind to CAR and appears to attach to DAF on the plasma membrane, which is in accordance with previous findings (Fig. 3) (23, 26, 27). To our surprise, however, siRNA knock-down of DAF did not prevent the infection of E30B, indicating that although DAF promotes E30B binding to cells, it is not needed for infection. In contrast, the siRNA knock-down of FcRn prevented E30B infection despite the fact that the distribution of the receptor in the cytoplasm did not appear to be affected by E30B infection, nor did it colocalize with the virus after entry. Taken together, these results suggest that while DAF may facilitate the binding of E30B on cells and may function as a co-receptor, the FcRn receptor is absolutely required for successful infection, which is in accordance with previous studies (28, 29).

Early endosomes function as cellular sorting stations which accumulate various uptake vesicles from the plasma membrane. Delivery of these vesicles can occur via different routes, some of which can be hijacked by viruses to facilitate their entry into the host cell. The increased colocalization of E30B with both EEA1 and transferrin suggests that E30B does indeed accumulate in early endosomes. However, there were several lines of evidence to suggest that E30B does not use clathrin-dependent entry to early endosomes. First of all, inhibition of dynamin had no effect on infectivity. Second, the entry to the early endosomes took longer than the typical clathrin cargos, which accumulate in early endosomes within minutes. In addition, expression of the dominant-negative small GTPase Rab5 construct decreased E30B infection. Furthermore, transfection of a constitutively active Rab5 construct increased E30B infection, suggesting that an increased amount of homotypic fusion of early endosomes, and supposedly with other incoming vesicles, promoted E30B infection (Fig. 11). This led us to believe that E30B can make use of early endosomes, but does not rely on clathrin-dependent entry to facilitate its entry into these organelles.

In addition to entry, the results suggested that the progression of infection was not dependent on acidification, which is typical for the clathrin-dependent pathway. This was proven by the lack of an inhibitory effect of bafilomycin A1. Furthermore, the absence of an effect with nocodazole suggests there is no explicit need for endosomal acidification, microtubule transport to perinuclear regions and late endosomes, or recycling of early endosomes to establish infection. The results thus altogether indicate that entry into early endosomal structures occurs not via clathrin-coated pits, but rather through cholesterol-containing raft domains, following a longer route to reach its destination.

270

271

272

273

274

275

276

277

278 279 280

281

282

283

284 285

286

287

288

289

290

291

292

293

294

295 296

297

298

299

300

301

302

303

304

305

306

307

308

In conclusion, E30B proved to be a typical enterovirus by not relying on acidification to ensure infection. E30B showed a preference for DAF over CAR for cellular attachment, but demonstrated the Fc receptor to be an absolute requirement for infection. In contrast to EV1 and CVA9, E30B depends on sorting to early endosomes for efficient uncoating and infection. This study represents, to the best of our knowledge, the first in-depth examination of E30B early entry and virus-host cell interaction mechanics. The development of a viable, efficiently replicating E30B clone enables examination of the virus's life cycle and its behaviour in vitro, opening the door to the development of better treatment strategies and care.

### **MATERIALS & METHODS**

Cells and viruses. Human RD and A549 cell lines, as well as CHO and GMK cells, were purchased from the American Tissue Culture Collection (ATCC). Additionally, two distinct lines of recombinant CHO cells (stably expressing human Coxsackie and Adenovirus receptor (CHO-CAR) and human Decay Accelerating Factor (CHO-DAF), respectively) were previously constructed by H. C. Selinka (37). Cells were maintained in Dulbecco's Modified Eagle's Medium (DMEM, Sigma-Aldrich) supplemented with 10 % fetal bovine serum (FBS, Sigma-Aldrich), 1 % penicillin-streptomycin and 2 mM L-glutamine (Sigma-Aldrich) at 37 °C, 5.0 % CO<sub>2</sub>.

An E30B infectious clone was designed using the prototype E30 Bastianni seguence (GenBank accession no AF311938.1) and subsequently produced and cloned into a pUC57 cloning vector (GenScript). A previously described hammerhead ribozyme structure containing an inactivated Ascl restriction enzyme site (G39C and C48G) was added at the 5' UTR, as well as a 28 A residue poly(A) tail at the 3' UTR (38). The plasmid was introduced into NovaBlue competent cells, which were incubated in LB-medium (1 % tryptone, 0.5 % yeast extract, 0.5 % NaCl) and plated on LB/Amp (100 µg/ml ampicillin) plates. Plasmid DNA was isolated and purified using the GeneJET Plasmid Miniprep Kit (Life Sciences).

Downloaded from http://jvi.asm.org/ on April 15, 2020 at KIRJASTO KAUSIJULKAISUT

**Transfection, virus production and purification.** RD cells were grown in a 6-well plate to 70 – 90 % confluence, transfected with E30B-pUC57 using Lipofectamine 2000 transfection reagent (InvitroGen), and incubated at 37 °C until complete cytopathic effect (CPE) was observed. Following transfection, cells were subjected to three rounds of freeze-thawing to ensure maximal virus yield, and generated viruses were further propagated through five serial passages to ensure adequate adaptation to the cell line. For each passage, 1.0 ml of lysate from either the transfection or the previous passage was added to subconfluent RD cells grown in a T25 flask, which was subsequently incubated for 1 h at room temperature. After incubation, the inoculum was removed, fresh cell medium was applied, and cells were further cultured at 37 °C until CPE was visible, or for a maximum of 5 days. To obtain purified virus, E30B was propagated in 5-layer flasks containing RD cells and subsequently purified using sucrose gradients as previously described (39). Cell culture medium for virus propagation and purification consisted of serum-free DMEM (Sigma-Aldrich) supplemented with 1 % penicillinstreptomycin and 2 mM L-glutamine (Sigma-Aldrich).

Downloaded from http://jvi.asm.org/ on April 15, 2020 at KIRJASTO KAUSIJULKAISUT

Transmission electron microscopy. Transmission electron microscopy (TEM) imaging was performed as previously described (40). Briefly, Butwar-coated copper grids were hydrophylised through glow discharging with an EMS/SC7620 Mini Sputter Coater (Quorum Technologies) as per the manufacturer's instructions before incubation with E30B for 15 s. Excess virus was removed, after which the remaining virions were negatively stained by incubating the grid with 1 % phosphotungstic acid in water (pH 7.4) for 1 min. After incubation, excess stain was removed and E30B (subjected to 5 min of heat treatment at 50 °C prior to application) was added. Samples were dried overnight and subsequently evaluated using a JEM-1400 transmission electron microscope (JEOL).

317 318 319

320

321

322

323

324

325

326

327

328

329 330

331

332

333 334

335

309 310

311

312

313

314

315

316

Confocal immunofluorescence imaging. RD and A549 cells were cultured on coverslips to subconfluency, washed once with PBS, and subsequently infected with E30B. After incubation at 37 °C, the cells were fixed at selected time points using 4 % paraformaldehyde (PFA) for 20 min, permeabilised using 0.2 % Triton X-100 for 5 min, and antibody labeled. The samples were mounted using Mowiol (Sigma-Aldrich) containing DABCO (1,4-diazabicyclo[2,2,2]octane, Sigma-Aldrich) and evaluated using an Olympus FluoView 1000 Laser Scanning Confocal Microscope or Leica SP8 with Leica's Lighting optimized settings using a voxel size of 35 nm in XY and 245 nm in Z.

The following antibodies were used: mouse monoclonal antisera against enterovirus VP1 capsid protein (cat. n° M7064, Dako), mouse monoclonal antisera against human EEA1 (cat. n° 610457, BD Biosciences), and mouse monoclonal antisera against dsRNA (J2, cat. n° 10010200, SCICONS); rabbit monoclonal antisera against Fc receptor (CD64, cat. nº ab193148, Abcam) and rabbit polyclonal antisera against EEA1 (cat. n° ab2900, Abcam); rhesus monkey monoclonal antiserum against human echovirus 30 (cat. n° VR-1072 AS/MK, ATCC); Alexa Fluor 488 goat polyclonal IgG against mouse (cat. n° A-11029, ThermoFisher Scientific); Alexa Fluor 555 goat polyclonal IgG against mouse (cat. n° A-21422, ThermoFisher Scientific); Alexa Fluor 488 goat polyclonal IgG against rabbit (cat. n° A-11008, ThermoFisher Scientific); Alexa Fluor 555 goat polyclonal IgG against rabbit (cat. n° A-21428, ThermoFisher Scientific); Alexa Fluor 647 goat polyclonal IgG agains rhesus monkey (cat. n° 6200-31, SouthernBiotech). Antibody dilutions were prepared in 3 % bovine serum albumin (BSA) in PBS.

336 337 338

> 339 340

341

342

343 344

345 346

347

348

Receptor binding assay. Radioactive <sup>35</sup>S-labeled E30B was produced as previously described (40). Briefly, RD monolayers were grown to subconfluency, washed once with PBS, and infected for 3 h at 37 °C with E30B diluted in low methionine/cysteine medium supplemented with 1 % FBS (Sigma-Aldrich). After incubation, the medium was replaced with low methionine/cysteine medium supplemented with 1 % FBS and 50 μCi/ml of [35S] methionine-cysteine (EasyTag EXPRESS 35S Protein Labeling Mix [35S], PerkinElmer) and infection was allowed to continue for 9 h at 37 °C. Cell lysates were collected after repeated freeze-thaw cycles, after which cell debris was pelleted through centrifugation at 4 °C using an SL-16R rotor (2,500 × g for 10 min, ThermoFisher Scientific). The supernatant was incubated with 0.3 % (wt/vol) sodium deoxycholate (DOC) and 0.6 % (vol/vol) Nonidet P-40 (NP-40) substitute for 30 min on ice. Membrane structures were pelleted through centrifugation at 4 °C using an SL-16R rotor (4,000 × g for 10 min) and the supernatant was applied to 40 % sucrose cushions. Samples were ultracentrifuged at 4 °C using an SW-41 rotor (35,000 rpm for 2.5 h, Beckman Coulter). The liquid above each cushion as well as one 500 µl fraction was discarded, while three subsequent 500 µl fractions were collected and applied to 5 - 20 % continuous sucrose gradients. Gradients were subjected to centrifugation at 4 °C using an SW-41 rotor (35,000 rpm for 2 h) and fractioned into 500 µl aliquots starting from the top, which were consequently analyzed through addition of 4 ml of Ultima Gold MV scintillation cocktail (PerkinElmer) and application of the Liquid Scintillation Analyzer Tri-Carb 2910 TR scintillation counting method (PerkinElmer).

CHO cells stably transfected with CAR (CHO-CAR) or DAF (CHO-DAF) were tested for strong DAF or CAR expression by immunofluorescence and FACS. Each adherent cell culture was individually detached using trypsin (Sigma-Aldrich) before 150,000 cells per replicate were washed, resuspended in 2 mM MgCl-PBS, and subsequently incubated at 4 °C with 50,000 CPM of 35S-labeled E30B (corresponding to MOI 850). After 1 hour, cells were washed to remove unbound virions, resuspended in 4 ml of Ultima Gold MV scintillation cocktail (PerkinElmer), and analyzed using the Liquid Scintillation Analyzer Tri-Carb 2910 TR scintillation counting method (PerkinElmer).

362 363 364

365

366

367

368

369

370 371

372

349

350

351

352

353

354

355

356 357

358

359 360

361

siRNA transfections. A549 cells were reverse transfected using DharmaFECT transfection reagent (Horizon Discovery) according to the manufacturer's instructions. The pool of three target-specific siRNAs against CAR, DAF or FcRn (Santa Cruz) or AllStars negative control siRNA (kindly gifted by the Johanna Ivaska laboratory, University of Turku, Turku, Finland) were added in a final concentration of 11.4 nM and the transfection was allowed to proceed for 48 h at 37 °C in DMEM supplemented with 10 % FBS and 1 % GlutaMax. Next, 200 PFU/cell of E30B or coxsackievirus B5 (CVB5) were added in DMEM supplemented with 1 % FBS and 1 % GlutaMax and bound on ice for 1 h after which the excess virus was washed away (41). The infection was then allowed to proceed at 37 °C in DMEM supplemented with 10 % FBS, 1 % GlutaMax for 6 h after which the cells were collected into 2 X Laemmli buffer containing β-mercaptoethanol.

Downloaded from http://jvi.asm.org/ on April 15, 2020 at KIRJASTO KAUSIJULKAISUT

373 374 375

376

377

378

379

380

381

382

SDS-PAGE and Western blot. The samples were boiled and separated in a 4-20% Mini-PROTEAN TGX Stain-Free gel (BioRad). Next, the proteins were transferred to PVDF membranes (Millipore) and blocked overnight with 5 % BSA and 0.05 % Tween in TBS. Blots were immunolabeled with mouse monoclonal antisera against enterovirus VP1 capsid protein (cat. n° M7064, Dako), and mouse monoclonal antisera against γ-tubulin (Abcam) was used as a loading control. The primary antibodies were detected using corresponding horseradish peroxidase-conjugated secondary antibodies (Cell Signaling), Finally, the chemiluminescent substrate SuperSignal West Pico PLUS (ThermoFisher Scientific) was incubated for 5 min and chemiluminescence was detected using the ChemiDoc MP (BioRad).

383 384 385

386

387

388

Pharmacological inhibitor assay. RD cells were cultured on coverslips to subconfluency. The cells were washed once with PBS and subsequently incubated at 37.0 °C in DMEM supplemented with 50.0 nM Bafilomycin A1 (targeting vacuolar type H<sup>+</sup> – ATPase, cat. n° 196000, Calbiochem), 33.0 μM Nocodazole (affecting microtubule assembly/disassembly, cat. n° 487928, Calbiochem), 100.0 µM Wortmannin (inhibiting phosphoinositide 3-kinase, cat. nº 681675, Calbiochem), 1.0 mM NSC 23766 (targeting Rac1, cat. n° 2161, Tocris BioScience), 10.0 µM U-73122 (affecting phospholipase C, cat. n° 662035, Calbiochem), or 12.5 µM Dyngo 4a (inhibiting dynamin, cat. n° 120689, Abcam) for 30 min prior to E30B addition (18). The infection assay was carried out for 6 h at 37 °C, after which the cells were fixed using 4 % PFA for 20 min, antibody labeled, and the presence of virus capsid protein was determined.

The cellular toxicity of the pharmacological inhibitors was evaluated using the CellTiter-Glo Luminescent Cell Viability Assay (Promega) according to the manufacturer's protocol.

396 397 398

399

400

401

402

403

404

405

406

407

408

409 410

411 412

413 414

415

389

390

391

392

393

394

395

Filipin assay. RD cells were cultured until subconfluency and incubated for 30 min with a 1, 2 or 3 µg/ml concentration of Filipin III (cat n° F4767, Sigma-Aldrich). Next, E30B was added onto the cells (200 PFU/cell) and bound on ice for 1 h after which excess virus was washed away. The infection was allowed to proceed for 6 h in DMEM supplemented with 10 % FBS, 1 % penicillin-streptomycin and 1 % GlutaMax, also including 1, 2 or 3 µg/ml of filipin. Finally, the medium was removed and viral RNA was isolated from lysed cells using the QIAamp Viral RNA extraction kit (Qiagen) according to the manufacturer's instructions. Reverse transcription was carried out for positive-sense RNA using 1.2 µM antisense primer (5'-GAAACACGGACACCCAAAGTA-3'), 20 U M-MLV Reverse Transcriptase (Promega), dNTPs (Promega) and 4 U RNasin Ribonuclease Inhibitor (Promega). 5 μl from the 40 μl reaction mixture was subsequently used in a PCR reaction which also included SYBR Green Supermix (BioRad) and 600 nM of both antisense primer (5'-GAAACACGGACACCCAAAGTA-3') and sense primer (5'-CGGCCCTGAATGCGGCTAA-3'). The amplification was carried out on the C1000 Touch Thermal Cycler with CFX96 Touch Real-Time PCR Detection System (BioRad) using the following protocol: 95 °C for 10 min; 40 cycles of 95 °C for 15 s to 60 °C for 1 min; and final melting step at 72 to 95 °C, 1 °C / 5 s. The assay also contained negative controls to confirm the specificity of

The cytotoxicity of filipin was evaluated using the CellTiter-Glo Luminescent Cell Viability Assay (Promega) according to the manufacturer's protocol.

416 417

418

419

420

421

422

423

424

425

426 427

428

Quantification of viral infection. Viral RNA was extracted from infected RD cell cultures using the QIAamp Viral RNA extraction kit (Qiagen) according to the manufacturer's protocol and subsequently copied to cDNA using the TaqMan Reverse Transcription Reagents kit (Applied Biosystems). Twostep qRT-PCR reactions were carried out on the 7500 Real-Time PCR System (Applied Biosystems) with 7500 SDS analysis software. Each reaction was prepared using 1 µl cDNA, 1 X Power SYBR Green Master Mix (Applied Biosystems), and 200 nM each of primers 5UTR-F (5'-CGTTGCGGAGTGTTTCGTTC-3') and 5UTR-R (5'-TCCGCAGTTAGGATTAGCCG-3') directed against the 5' UTR of the genome in a final reaction volume of 20 µl. The following thermocycling program was applied: reverse transcription at 50 °C for 2 min, Tagman<sup>®</sup> DNA polymerase activation and simultaneous reverse transcriptase inactivation at 95 °C for 10 min, followed by 40 cycles of 15 s. at 95 °C and 60 s. at 60 °C. Each reaction was run in triplicate. Standard curves were generated by running the aforementioned protocol using the E30B cDNA template in triplicate.

Transferrin - EEA1 assay. RD cells were cultured on coverslips to subconfluency, washed once with PBS, and incubated with purified E30B or CVA9 (Griggs strain) for 1 h on ice. After virus binding, the medium was removed, cells were gently washed with 0.5 % BSA - PBS, and 50 µg/ml of transferrin -Alexa Fluor 488 conjugate (transferrin from human serum, Alexa Fluor 488 conjugate, InvitroGen) in DMEM supplemented with 0.2 % BSA was added. Infection was carried out at 37 °C and terminated at 5 min and 30 min timepoints by fixing the cells with 4 % PFA for 20 min, after which the cells were antibody labeled and imaged.

436 437 438

439

440

441

442

443

444

445

446

447

448

449 450

429 430

431

432

433

434

435

Plasmid transfections. RD cells were grown on coverslips to subconfluency. Plasmid transfections were carried out for 48 h at 37 °C using Lipofectamine 3000 transfection reagent (InvitroGen) according to the manufacturer's instructions. The cells were infected with 200 PFU/cell of E30B or CVA9 (Griggs strain) by binding the virus on ice for 1 h in DMEM supplemented with 1 % FBS and 1 % GlutaMax. After excess virus was washed away, the infection was allowed to proceed for 6 h at 37 °C in DMEM supplemented with 10 % FBS, 1 % GlutaMax, and 1 % penicillin-streptomycin. Finally, the cells were fixed using 4 % PFA for 20 min and labeled with mouse monoclonal antisera against enterovirus VP1 capsid protein (cat. nº M7064, Dako). The infection percentage of transfected cells was quantified by evaluating the presence of viral capsid protein.

Plasmid constructs were obtained from the following sources: the dominant-negative (pEGFP-Rab5-S34N) and dominant-positive (pEYFP-Rab5-Q79L) Rab5 constructs were procured from Lucas Pelkmans (Department of Molecular Life Sciences, University of Zurich, Zurich, Switzerland), and the wild type Rab5 (pEGFP-Rab5) was acquired from Miguel Seabra (Faculty of Medicine, National Heart and Lung Institute, Imperial College, London, United Kingdom).

Downloaded from http://jvi.asm.org/ on April 15, 2020 at KIRJASTO KAUSIJULKAISUT

451 452 453

454

455

456 457

458

459 460 Microscopy data analysis. Microscope settings were optimised for each channel prior to imaging. Confocal immunofluorescence image analysis was executed using the Fiji free open source software package (42). For the colocalization analysis, the coloc2 plugin was used to measure the Manders' correlation and Costes' significance with a PSF estimation of 8 pixels and 20 iterations (43, 44). Image analysis was executed using the Fiji free open source software package (42). To visualize colocalizing pixels between transferrin, EEA1 and E30B or CVA9 (Griggs strain) the open source software BioImageXD (www.bioimagexd.net) was used. Thresholding for E30B was set with the help of uninfected controls, and for transferrin and EEA1 they were set manually, to not contain background signal.

461 462 463

464

465

Statistical analysis. Statistical sample comparison of proportions and ratios was performed using an arcsine square root transformation to convert the data to be more normally distributed, followed by a paired or unpaired t-test. A p-value of < 0.05 was considered statistically significant.

### **ACKNOWLEDGEMENTS**

466 467

469

470

471

472

473 474

Jyväskylä, Jyväskylä, Finland) for technical assistance.

**CONFLICTS OF INTEREST** 

None to declare.

We would like to thank Kjell Edman (Linnaeus Univerisity, Kalmar, Sweden) for valuable discussions

and technical assistance. We would also like to acknowledge Sami Salmikangas (University of

Downloaded from http://jvi.asm.org/ on April 15, 2020 at KIRJASTO KAUSIJULKAISUT

### **REFERENCES**

476

475

- 477 Irani DN. 2008. Aseptic meningitis and viral myelitis. Neurol Clin 26:635-655. 1.
- 2. Khetsuriani N, Quiroz ES, Holman RC, Anderson LJ. 2003. Viral meningitis-associated 478 479 hospitalizations in the United States, 1988-1999. Neuroepidemiology 22:345-352.
- 480 Pallansch MA, Roos RP. 2007. Enteroviruses: polioviruses, coxsackieviruses, echoviruses, and 481 newer enteroviruses, p 839-893. In Knipe DM, Howley PM (ed), Fields Virology, 5th ed, vol 1.
- 482 Lippincott Williams & Wilkins, a Wolters Kluwer business, Philadelphia, USA.
- Connolly KJ, Hammer SM. 1990. The acute aseptic meningitis syndrome. Infect Dis Clin North 483 484 Am 4:599-622.
- 485 Control 5. Centers for Disease and Prevention (CDC). 2016. Viral meningitis. 486 https://www.cdc.gov/meningitis/viral.html. Accessed 03 Dec 2018.
- 487 6. Rotbart HA. 2000. Viral meningitis. Semin Neurol 20:277-292.
- 488 7. Davidson KL, Ramsay ME. 2003. The epidemiology of acute meningitis in children in England 489 and Wales. Arch Dis Child 88:662-664.
- 490 Logan SA, MacMahon E. 2008. Viral meningitis. BMJ 336:36-40.
- 491 Yamashita K, Miyamura K, Yamadera S, Kato N, Akatsuka M, Hashido M, Inouye S, Yamazaki S.
- 492 1994. Epidemics of aseptic meningitis due to echovirus 30 in Japan. A report of the National 493 Epidemiological Surveillance of Infectious Agents in Japan. Jpn J Med Sci Biol 47:221-239.
- 494 10. Oberste MS, Maher K, Kennett ML, Campbell JJ, Carpenter MS, Schnurr D, Pallansch MA. 1999.
- 495 Molecular epidemiology and genetic diversity of echovirus type 30 (E30): genotypes correlate 496 with temporal dynamics of E30 isolation. J Clin Microbiol 37:3928-3933.
- 497 11. Thoelen I, Lemey P, Van Der Donck I, Beuselinck K, Lindberg AM, Van Ranst M. 2003. Molecular 498 typing and epidemiology of enteroviruses identified from an outbreak of aseptic meningitis in
- 499 Belgium during the summer of 2000. J Med Virol 70:420-429.
- 12. Centers for Disease Control and Prevention (CDC). 2003. Outbreaks of aseptic meningitis 500 501 associated with echoviruses 9 and 30 and preliminary surveillance reports on enterovirus 502 activity—United States, 2003. MMWR Morb Mortal Wkly Rep 52:761-764.
- 503 13. Centers for Disease Control and Prevention (CDC). 2006. Enterovirus surveillance-United 504 States, 2002-2004. MMWR Morb Mortal Wkly Rep 55:153-156.
- 505 14. McWilliam Leitch EC, Bendig J, Cabrerizo M, Cardosa J, Hyypiä T, Ivanova OE, Kelly A, Kroes AC, Lukashev A, MacAdam A, McMinn P, Roivainen M, Trallero G, Evans DJ, Simmonds P. 506 507 2009. Transmission networks and population turnover of echovirus 30. J Virol 83:2109-2118.
- 508 15. Broberg EK, Simone B, Jansa J, The EU/EEA Member State Contributors. 2018. Upsurge in 509 echovirus 30 detections in five EU/EEA countries, April to September, 2018. Euro Surveill 23.
- 510 16. Oberste MS, Maher K, Kilpatrick DR, Pallansch MA. 1999. Molecular evolution of the human 511 enteroviruses: correlation of serotype with VP1 sequence and application to picornavirus 512 classification. J Virol 73:1941-1948.
- 513 17. Diedrich S, Driesel G, Schreier E. 1995. Sequence comparison of echovirus type 30 isolates to 514 other enteroviruses in the 5' noncoding region. J Med Virol 46:148-152.

- 515 18. Huttunen M, Waris M, Kajander R, Hyypiä T, Marjomäki V. 2014. Coxsackievirus A9 infects cells 516 via nonacidic multivesicular bodies. J Virol 88:5138-5151.
- 517 19. Pietiäinen V, Marjomäki V, Upla P, Pelkmans L, Helenius A, Hyypiä T. 2004. Echovirus 1 518 endocytosis into caveosomes requires lipid rafts, dynamin II, and signaling events. Mol Biol Cell 519 15:4911-4925.
- 520 20. Bergelson JM, Cunningham JA, Droguett G, Kurt-Jones EA, Krithivas A, Hong JS, Horwitz MS, 521 Crowell RL, Finberg RW. 1997. Isolation of a common receptor for coxsackie B viruses and 522 adenoviruses 2 and 5. Science 275:1320-1323.
- 523 21. Martino TA, Petric M, Weingartl H, Bergelson JM, Opavsky MA, Richardson CD, Modlin JF, 524 Finberg RW, Kain KC, Willis N, Gauntt CJ, Liu PP. 2000. The coxsackie-adenovirus receptor 525 (CAR) is used by reference strains and clinical isolates representing all six serotypes of 526 coxsackievirus group B and by swine vesicular disease virus. Virology 271:99-108.
- 527 22. Marjomäki V, Turkki P, Huttunen M. 2015. Infectious entry pathway of enterovirus B species. 528 Viruses 7:6387-6399.
- 529 23. Bergelson JM, Chan M, Solomon KR, St John NF, Lin H, Finberg RW. 1994. Decay-accelerating 530 factor (CD55), a glycosylphosphatidylinositol-anchored complement regulatory protein, is a 531 receptor for several echoviruses. Proc Natl Acad Sci U S A 91:6245-6248.
- 532 24. Shafren DR, Bates RC, Agrez MV, Herd RL, Burns GF, Barry RD. 1995. Coxsackieviruses B1, 533 B3, and B5 use decay accelerating factor as a receptor for cell attachment. J Virol 69:3873-3877.
- 534 25. Milstone AM, Petrella J, Sanchez MD, Mahmud M, Whitbeck JC, Bergelson JM. 2005. Interaction 535 with coxsackievirus and adenovirus receptor, but not with decay-accelerating factor (DAF), 536 induces A-particle formation in a DAF-binding coxsackievirus B3 isolate. J Virol 79:655-660.
- 537 26. Powell RM, Schmitt V, Ward T, Goodfellow I, Evans DJ, Almond JW. 1998. Characterization of 538 echoviruses that bind decay accelerating factor (CD55): evidence that some haemagglutinating strains use more than one cellular receptor. J Gen Virol 79:1707-1713. 539
- 540 27. Rothe D, Werk D, Niedrig S, Horbelt D, Grunert HP, Zeichhardt H, Erdmann VA, Kurreck J. 2009. 541 Antiviral activity of highly potent siRNAs against echovirus 30 and its receptor. J Virol Methods 542 157:211-218.
- 543 28. Morosky S, Wells AI, Lemon K, Evans AS, Schamus S, Bakkenist CJ, Coyne CB. 2019. The 544 neonatal Fc receptor is a pan-echovirus receptor. Proc Natl Acad Sci U S A 116:3758-3763.
- 545 29. Zhao X, Zhang G, Liu S, Chen X, Peng R, Dai L, Qu X, Li S, Song H, Gao Z, Yuan P, Liu Z, Li C, 546 Shang Z, Li Y, Zhang M, Qi J, Wang H, Du N, Wu Y, Bi Y, Gao S, Shi Y, Yan J, Zhang Y, Xie Z,
- Wei W, Gao GF. 2019. Human neonatal Fc receptor is the cellular uncoating receptor for 547 548 enterovirus B. Cell 177:1553-1565.
- 549 30. Triantafilou K, Triantafilou M. 2004. Lipid-raft-dependent coxsackievirus B4 internalization and 550 rapid targeting to the Golgi. Virology 326:6-19.
- 31. Patel KP, Coyne CB, Bergelson JM. 2009. Dynamin- and lipid raft-dependent entry of decay-551 552 accelerating factor (DAF)-binding and non-DAF-binding coxsackieviruses into nonpolarized cells. 553 J Virol 83:11064-11077.

Downloaded from http://jvi.asm.org/ on April 15, 2020 at KIRJASTO KAUSIJULKAISUT

586

- 554 32. Krieger SE, Kim C, Zhang L, Marjomaki V, Bergelson JM. 2013. Echovirus 1 entry into polarized 555 Caco-2 cells depends on dynamin, cholesterol, and cellular factors associated with 556 macropinocytosis. J Virol 87:8884-8895.
- 557 33. Marjomäki V, Pietiäinen V, Matilainen H, Upla P, Ivaska J, Nissinen L, Reunanen H, Huttunen P, 558 Hyypiä T, Heino J. 2002. Internalization of echovirus 1 in caveolae. J Virol 76:1856-1865.
- 559 34. Bucci C, Parton RG, Mather IH, Stunnenberg H, Simons K, Hoflack B, Zerial M. 1992. The small 560 GTPase Rab5 functions as a regulatory factor in the early endocytic pathway. Cell 70:715-728.
- 35. Feliciano WD, Yoshida S, Straight SW, Swanson JA. 2011. Coordination of the Rab5 cycle on 561 562 macropinosomes. Traffic 12:1911-1922.
- 563 36. Egami Y, Taguchi T, Maekawa M, Arai H, Araki N. 2014. Small GTPases and phosphoinositides 564 in the regulatory mechanisms of macropinosome formation and maturation. Front Physiol 5:374.
- 565 37. Selinka HC, Wolde A, Pasch A, Klingel K, Schnorr JJ, Küpper JH, Lindberg AM, Kandolf R. 2002. 566 Comparative analysis of two coxsackievirus B3 strains: putative influence of virus-receptor 567 interactions on pathogenesis. J Med Virol 67:224-233.
- 568 38. Israelsson S, Sävneby A, Ekström JO, Jonsson N, Edman K, Lindberg AM. 2014. Improved replication efficiency of echovirus 5 after transfection of colon cancer cells using an authentic 5' 569 570 RNA genome end methodology. Invest New Drugs 32:1063-1070.
- 571 39. Abraham G, Colonno RJ. 1984. Many rhinovirus serotypes share the same cellular receptor. J 572 Virol 51:340-345.
- 573 40. Myllynen M, Kazmertsuk A, Marjomäki V. 2016. A novel open and infectious form of echovirus 1. 574 J Virol 90:6759-6770.
- 575 41. Turkki P, Laajala M, Stark M, Vandesande H, Sallinen-Dal Maso H, Shroff S, Sävneby A, Galitska 576 G, Lindberg AM, Marjomäki V. 2019. Slow infection due to lowering the amount of intact versus 577 empty particles is a characteristic feature of coxsackievirus B5 dictated by the structural proteins. 578 J Virol 93.
- 579 42. Schindelin J, Arganda-Carreras I, Frise E, Kaynig V, Longair M, Pietzsch T, Preibisch S, Rueden 580 C, Saalfeld S, Schmid B, Tinevez JY, White DJ, Hartenstein V, Eliceiri K, Tomancak P, Cardona 581 A. 2012. Fiji: an open-source platform for biological-image analysis. Nat Methods 9:676-682.
- 43. Manders EMM, Verbeek FJ, Aten JA. 1993. Measurement of co- localization of objects in dual-582 583 colour confocal images. J Microsc 169:375-382.
- 44. Costes SV, Daelemans D, Cho EH, Dobbin Z, Pavlakis G, Lockett S. 2004. Automatic and 584 585 quantitative measurement of protein-protein colocalization in live cells. Biophys J 86:3993-4003.

### FIGURE LEGENDS

588

587

589

590

591

592

593

594

595

596

597

FIG. 1. E30B displays efficient replication and infection kinetics. (A, B) Transmission electron microscope imaging of purified virus particles. Scale bars are 500 nm (A) and 100 nm (B). (C) Immunofluorescence staining of RD cells, 2 h, 3 h and 7 h post-infection (p.i.) with E30B. The presence of double-stranded RNA (dsRNA) indicates viral replication. Red, dsRNA (J2); blue, nuclei (DAPI). Scale bar is 15 µm. (D) Time-resolved quantification of intracellular dsRNA accumulation in RD cells after E30B infection through measurement of the anti-dsRNA (J2) signal intensity. Results are presented as mean values of 12 areas containing 5 - 6 cells each (± standard error of the mean [SEM]) (E) Time-resolved quantitative RT-PCR following the intracellular accumulation of E30B RNA in RD cells. A high cycle threshold (C<sub>1</sub>) value corresponds to a low amount of intracellular viral RNA. Results are presented as mean values of 3 replicates (± standard deviation [SD]).

598 599

600 FIG. 2. Immunofluorescence staining of the E30B capsid in infected RD cells. Infected cells are marked with an asterisk (\*). Purple, VP1 capsid protein (antibody made in rhesus monkeys); blue, 601 602 nuclei (DAPI). Scale bar is 10 µm.

603 604

605

606 607 FIG. 3. E30B binding assay. 50,000 counts per minute (CPM) of metabolically labeled E30B was bound on ice to 150,000 CHO cells for 1 hour and washed. Results are presented as mean values of 3 replicates (± standard error of the mean [SEM]).CHO-cells stably transfected with CAR (CHO-CAR) or DAF (CHO-DAF) were tested for strong DAF or CAR expression by immunofluorescence and FACS (data not shown).

608 609 610

611

612

FIG. 4. Colocalization analysis of E30B and FcRn in A549 cells. Example of the localisation of E30B and FcRn signals from representative cells for each time point shown as a maximum intensity projection. The Manders' coefficient represents the percentage of E30B voxels colocalizing with the FcRn voxels.

613 614 615

616

617

618

619

620

FIG. 5. The effect of CAR, DAF and FcRn siRNA knock-down on E30B infection. A549 cells were transfected for 48 h with pooled siRNAs against CAR, DAF or FcRn or with negative control siRNA (CTRLsi) and infected with E30B or CVB5 for 6 h. Top, representative image of Western blot where the infection was detected by immunolabeling of VP1 and γ-tubulin as a loading control. Bottom, quantification of the infection from Western blots by normalizing the VP1 signal to  $\gamma$ -tubulin. Results are presented as mean values of 3 replicates (± standard error of the mean [SEM]). Statistical significance was determined using an unpaired t-test. \*, p < 0.05; \*\* p < 0.01; \*\*\* p < 0.001.

621 622 623

624

FIG. 6. Pharmacological inhibition of early E30B entry. Immunofluorescence staining of RD cells, 6 h post-infection (p.i.) with E30B. Cells were pretreated with inhibitory chemicals 30 min before addition of the virus. The presence of capsid indicates viral replication. Red, viral capsid (DAKO); blue, nuclei (DAPI). Scale bar is 20 µm.

627

625

626

628

629

FIG. 7. Cell viability assay of RD cells treated with pharmacological compounds. Cell viability measurement of RD cells, 6.5 h after treatment with indicated inhibitory chemicals. Results are presented as mean values of 6 replicates (± standard deviation [SD]). CTRL, untreated control cells.

630 631 632

633

634

635

636

637

FIG. 8. Pharmacological inhibition of early E30B entry. Quantitative RT-PCR measuring the intracellular accumulation of E30B RNA in RD cells treated with pharmacological inhibitors, 6 h postinfection (p.i.). Cells were pretreated with inhibitory chemicals 30 min before addition of the virus. A high cycle threshold (C<sub>1</sub>) value corresponds to a low amount of intracellular viral RNA. Results are presented as mean values of 3 replicates (± standard deviation [SD]). POS, positive control for infection without the presence of the vehicle; NEG, negative control for infection; DMSO: positive control for infection in the presence of the vehicle.

638 639 640

641

642

643

644

645

FIG. 9. The effect of the cholesterol modifying drug filipin on E30B infection. (A) Quantitative RT-PCR measuring the intracellular accumulation of E30B RNA in RD cells treated with different concentrations of the caveolae pathway inhibitor filipin, 6 h post-infection (p.i.). Results are presented as mean values of 3 replicates (± standard deviation [SD]). CTRL E30B, control infection without filipin. Statistical significance was determined using an unpaired t-test. \*\*\*\*, p < 0.0001. (B) Cell viability assay of RD cells after treatment with different filipin concentrations for 6 h. Results are presented as mean values of 3 replicates (± standard deviation [SD]). CTRL, untreated control cells.

Downloaded from http://jvi.asm.org/ on April 15, 2020 at KIRJASTO KAUSIJULKAISUT

646 647 648

649 650

651

FIG. 10. E30B colocalizes with early endosomes during early entry. E30, or CVA9 as a control, was bound to RD cells on ice, washed, and incubation was continued at 37 °C with transferrin - Alexa Fluor 488 for 5 or 30 min, after which cells were fixed and labeled also for EEA1. Green, transferrin receptor (transferrin - Alexa Fluor 488); red, early endosomal antigen (EEA1); purple, VP1 capsid protein (antibody made in rhesus monkeys). Scale bar is 10 µm.

652 653 654

655 656

657

658

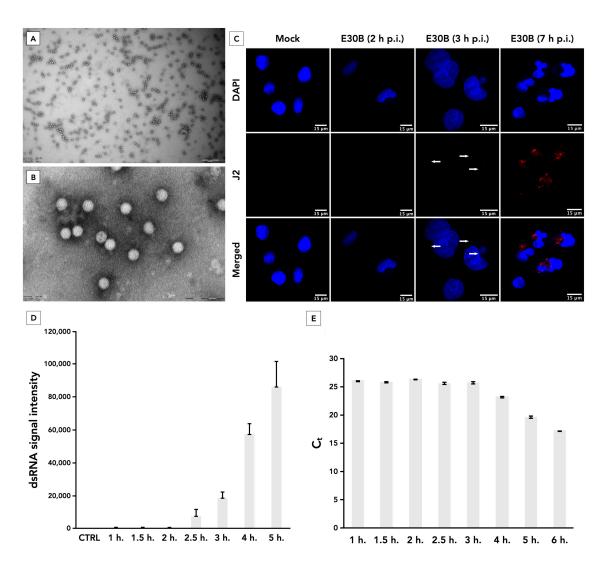
659

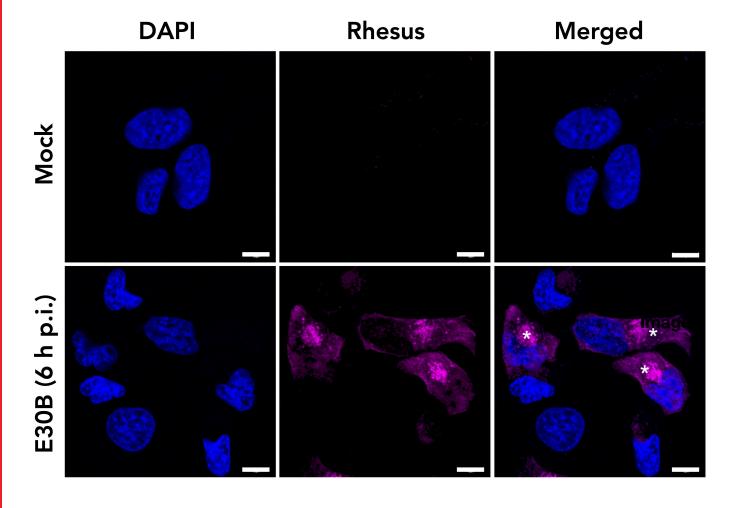
660

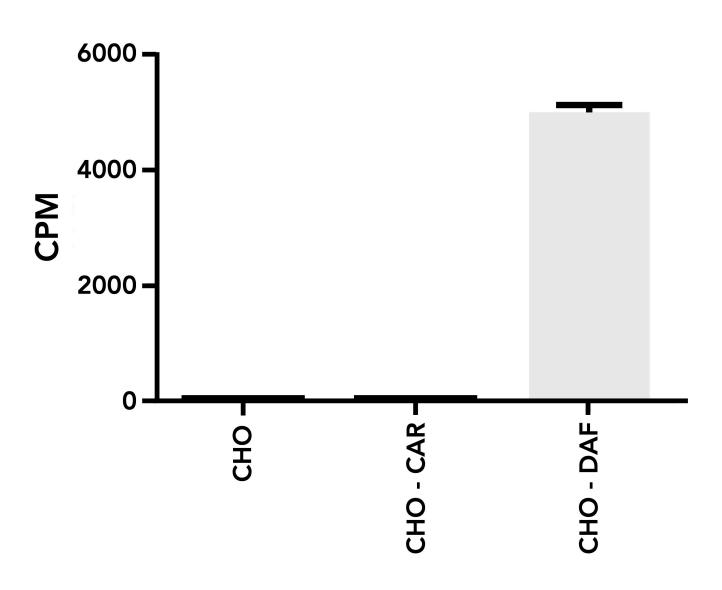
661

662

FIG. 11. The effect of Rab5 on E30B infection. RD cells were transfected with a wild type (pEGFP-Rab5-WT), a dominant-negative (pEGFP-Rab5-S34N) or a constitutively active (pEGFP-Rab5-Q79L) Rab5 construct. Cells and plasmids were incubated for 48 h to allow for stable expression, followed by infection for 6 h with E30B or CVA9, after which the infection was detected using immunofluorescence microscopy. The infection percentage of transfected cells was quantified based on VP1 signal, and 350-550 transfected cells were calculated per sample in total. Results are normalized to wild type control and presented as mean values of 3 replicates (± standard error of the mean [SEM]). Statistical significance was determined using an arcsine square root transformation followed by an unpaired ttest. \*, p < 0.05; \*\* p < 0.01.







Downloaded from http://jvi.asm.org/ on April 15, 2020 at KIRJASTO KAUSIJULKAISUT

